1 **Social Behaviour and Collective Motion in Plant-Animal Worms.**

2 Nigel R. Franks[1*], Alan Worley[1], Katherine A.J. Grant[1], Alice R. Gorman[1], Victoria
3 Vizard[1], Harriet Plackett[1], Carolina Doran[1], Margaret L. Gamble[1], Martin C. Stumpe[2],
4 Ana B. Sendova-Franks[3]

5 [1]School of Biological Sciences, University of Bristol, UK

6 [2]AnTracks Computer Vision Systems, Mountain View, CA, USA

7 [3]Department of Engineering Design and Mathematics, UWE, Bristol, UK

8 *corresponding author email: nigel.franks@bristol.ac.uk

9 **Abstract**

10 Social behaviour may enable organisms to occupy ecological niches that would

11 otherwise be unavailable to them. Here we test this major evolutionary principle by

12 demonstrating self-organizing social behaviour in the plant-animal, *Symsagittifera*

13 *roscoffensis*. These marine aceol flat worms rely for all of their nutrition on the algae

14 within their bodies: hence their common name. We show that individual worms

15 interact with one another to co-ordinate their movements so that even at low

16 densities they begin to swim in small polarized groups and at increasing densities

17 such flotillas turn into circular mills. We use computer simulations to: (1) determine if

18 real worms interact socially by comparing them with virtual worms that do not interact

19 and (2) show that the social phase transitions of the real worms can occur based

20 only on local interactions between and among them. We hypothesize that such

21 social behaviour helps the worms to form the dense biofilms or mats observed on

22 certain sun-exposed sandy beaches in the upper intertidal of the East Atlantic and to

23 become in effect a super-organismic seaweed in a habitat where macro-algal

24 seaweeds cannot anchor themselves. *S. roscoffensis*, a model organism in many

25 other areas in biology (including stem cell regeneration), also seems to be an ideal

26 model for understanding how individual behaviours can lead, through collective

27 movement, to social assemblages.

1. Introduction

The study of collective motion is rapidly becoming a major interdisciplinary field in its own right, bringing approaches from statistical physics to social behaviour [1]. This field, at its best, is characterized by cycles of modelling and experimentation on particular study systems that elucidate general principles applicable to, for example, shaken metallic rods through macromolecules, bacterial colonies, amoebae, cells, insects, fish, birds, mammals and human social behaviour [1]. One emergent concept in the field of collective motion is that with increasing density many flocking systems exhibit a series of phase transitions ranging from isolated individuals through small polarized groups to circular mills and finally static assemblages. In colloids and granular materials, the slowdown of movement with increasing density is known as jamming [2], a transition also observed in human panic evacuation [3]. Systems that exhibit all three of these phase transitions are, however, rare (but see recent work focussing on the last of these transitions in collective cellular movement during metazoan development [4] and reticulate pattern formation in cyanobacteria [5]). Here we test the idea that a new model system exhibits all three transitions.

Our study model is the marine flat aceol [6] worm *Symsagittifera roscoffensis* renowned as the plant-animal [7],[8]. Adult *S. roscoffensis* feed on the nutrients produced by the photosynthesizing symbiotic algae living within their bodies. Hence, they seek sites where their algae can photosynthesize [9] more effectively. These worms are typically encountered as biofilms on sandy beaches at low tide [8]. In initial observations of *S. roscoffensis* transferred at fairly high densities to petri dishes with a shallow pool of sea water, we noted a rapid and spontaneous emergence of circular milling behaviour, which, to the best of our knowledge, had not

2

been described before in these worms, very possibly because it may occur only

fleetingly at a certain stage of the tidal cycle, for example when *S. roscoffensis*

initially come to the surface on the beaches they inhabit. Hence, the purpose of this

paper is to test hypotheses, through cycles of experimentation and modelling, which

focus on the transitions in the social behaviour and collective motion of these worms.

We determine how individual worms move, how small groups of worms interact with

one another and how circular mills form. We propose that circular milling gathers

worms together and eventually leads to such high densities that the worms can form

continuous biofilms and thus act as if they are a super-organismic seaweed.

One of the most extreme manifestations of collective motion is circular milling. It

occurs when individuals in a group are so synchronized that they follow one another

nose-to-tail in a complete ring in such a way that their trajectories are almost

identical and approximately circular; often there are multiple orbits nested within one

another [10],[11]. At the outset of modern studies of collective decision-making,

circular milling behaviour was seen as a key characteristic of ultra-cohesive group

movement [10]. It has been reported, for example, in *Bacillus* bacteria [12],[13] ,

Daphnia [14], processionary caterpillars [15], army ants [16], fish [17],[18] and

tadpoles [19]. Mechanistically, circular milling typically occurs because an isolated

group of individuals follow one another in a continuous ring. In processionary

caterpillars and army ants, circular milling is underpinned by individuals laying trails

that others follow and reinforce [15],[16]. In fish, it occurs because of rules of

attraction and alignment [11],[20],[21],[22]. A recent sophisticated analysis of

collective motion in glass prawns demonstrates that a weak form of circular milling

can occur in an annular arena because these supposedly non-social Crustacea

influence one another's movements even after a substantial delay following an

77   encounter [23].

78   The functional significance of circular milling is much less clear. Indeed, circular

79   milling seems often to be maladaptive, especially in processionary caterpillars and

80   army ants where individuals may remain trapped in a mill, by more and more trail

81   laying, until they die of exhaustion [16]. In fish, where it occurs fairly frequently, it

82   may serve for predator avoidance [20] through an extreme form of the geometry for

83   the selfish herd [24]. By contrast, in glass prawns, confinement to a donut-shaped

84   environment facilitates interactions and generates collective circular motion [23]. In

85   general, however, explanations for circular milling remain elusive. The experimental

86   tractability of the social behaviour and collective motion in *S. roscoffensis* we

87   demonstrate here, promises to elucidate the reasons why circular milling occurs both

88   mechanistically and functionally in this species.

89   First, we examine the characteristics of individual worms including their sizes, their

90   speeds of movement and their behavioural lateralization. Second, we determine if

91   these worms have a tendency to interact even at low densities such that they

92   encounter and line up with one another more frequently than they would if oblivious

93   of others. To do this, we create the first of two computer simulation models to mimic

94   the densities, lengths, and rates of movement of real worms in arenas of the same

95   size and shape as used in our experiments with real worms. This first model

96   represents the null hypothesis of no social interaction. Hence, we use simulations of

97   this model to detect potential social behaviours among the real worms. Third, we

98   analyse the occurrence of circular milling as a function of worm density. Fourth,

99   having established through comparisons with the null-hypothesis model that real

100   worms do interact socially, even at low densities, we create the second model based

101 on worms having simple rules of local interactions. The simulations of this second

102 model reproduce the formation of small polarized groups of moving worms that lead,

103 at yet higher densities, to circular mills. Finally, we put forward the hypothesis that

104 the purpose of these circular mills is to enable the worms to congregate into

105 extremely high-density assemblages that then can become biofilms.

106 **2. Material and methods**

107 **(a) Study organisms and experimental videos**

108 We collected *S. roscoffensis* from a north-easterly-facing beach on the North East

109 Coast of Guernsey on 17th to 19th June 2014. The worms were held at ambient

110 temperature in seawater collected from the same site and transferred to arenas for

111 filming. The depth of water within each arena was approximately 2 mm and the

112 worms were swimming freely. Filming at 15fps with a Canon G7 camera using a

113 resolution of 768 by 1024 pixels per frame followed within minutes of collection to

114 minimise the length of time the worms were held. We made fourteen videos of a total

115 of 707 worms. Thirteen of the videos recorded the behaviour of between 3 and 99

116 worms in a circular ceramic arena ($2875mm^2$) for varying values at low density and

117 one recorded 293 worms in a square plastic weighing boat ($961mm^2$) for a high-

118 density value. The videos were between 164 and 792s in length.

119 **(b) Characteristics of individual worms**

120 For length measurements, we took still images, in which each worm could be seen

121 clearly, from a representative sample from four of the videos at low worm densities in

122 the circular arenas (excluding two videos with 61 and 99 worms). Using ImageJ

123 software [25] a straight line was drawn across the diameter of the arena in each

5

124   image to provide a length calibration. We then used the 'segmented line' freehand

125   drawing tool, and the 'fit spline' option to draw a line from end to end of the worm,

126   matching any curvature, to produce a data set of worm lengths in mm.

127   For individual trajectories, we tracked worms in their quasi-2D environment of a

128   shallow pool of seawater in other four videos at low density in the circular arenas

129   using the AnTracks software system [26]. From these trajectories we extracted

130   length, speed, curvature and handedness to test for any relationship between length

131   and speed, explore the effect of curvature on speed and investigate whether

132   individual behavioural lateralization influences the formation of circular mills.

133   **(c) Interactions between worms: frequency**

134   We used the same interval of 2s (see later for justification) for the analysis of the

135   videos and their paired simulations to minimize any issues of pseudo-replication. As

136   the speeds of the worms in the videos and in the simulations were similar, the

137   chance that the same interactions would be seen in successive frames would be

138   similar, all else being equal, in both the videos and the simulations. Rather than

139   using automated methods to detect worm encounters in the simulations, we used the

140   same human observers to detect interactions both in the simulations and in the

141   experimental videos. It was not difficult for a human observer to count the well-

142   defined crossing and polarization events (see later) on still video frames and

143   simulation bitmap images. Hence, this very simple procedure ensured that the same

144   criteria were applied to both and hence that the difference between them was

145   reproducible.

146   *(i) Experimental videos*

147 The software 'ImageGrab' (http://imagegrab.en.softonic.com/, accessed October

148 2014) was used to take a still image from the videos every 2s. This interval was

149 chosen to avoid counting the same interaction twice because in 2s worms on

150 average moved approximately two body lengths (average length = 1.68mm, see

151 Results; average speed = 1.78mms^{-1}, see figure S1). The images were then

152 analysed one by one for the number of interactions. We recognized two types of

153 interaction: (1) crossing – two worms are in direct contact but are not aligned in the

154 same direction, that is, one is crossing over the other (the vertical proximity is

155 approximately 1mm, given the approximately 0.5 mm diameter of the worms and the

156 2mm water depth); (2) polarization – two worms are swimming in the same direction

157 and orientation, in close proximity (within 1mm), and in parallel or tandem positions.

158 Such close proximity (within 1mm) is almost certain to involve interaction even if only

159 owing to disturbance in the physical environment.

160 Each contact between any two or more worms was counted. Therefore, if a worm

161 had a worm parallel to it on either side, two polarized interactions were counted;

162 similarly if there were two worms swimming next to each other, and one was also

163 crossing over with a third worm, one crossing and one polarization interaction were

164 recorded. The total number of each interaction type was counted for each video and

165 then divided by the number of analysed images to calculate an average number of

166 interactions per image for a video. The analysis was based on 11 videos (figure

167 1*c*&*d*). The videos of the circular arena with 61 and 99 worms and of the square

168 arena with 293 worms were not included because such high densities made these

169 observations more difficult.

170 *(ii) Simulation of non-interacting worms*

171 The swimming behaviour of individual *S. roscoffensis* worms was recreated by

172 computer simulation. The scale of the simulation was the same as that of the

173 experimental video and the number of worms, and their lengths, were chosen to

174 match specific videos. The worms were made up of 0.2mm units, which moved

175 through the removal of a unit at the tail end and the replacement of it at the head

176 end, each time changing the head-end angle by up to +/- 0.1 rad using a uniform

177 distribution.

178 The simulation was configured so that it would run for the same length of time as the

179 corresponding video and had an option to save bitmaps at set intervals. This function

180 was used to collect the screenshots that were analysed. The worms were produced

181 in six colours, and had a black dot at the leading or 'head' end to aid in identifying the

182 direction of movement during analysis (e.g. to determine polarized events).

183 The simulation used realistic worm lengths and densities to replicate each video. The

184 bitmap interval was set to 2s and the number of frames entered so that the

185 simulation run time would match the duration of each video as in **(c)** *(i)*.

186 For each image the number of crossings and polarization events were recorded, the

187 different colours of the worms aided counting the number of worms involved in each

188 event, and the black heads helped to differentiate between parallel worms travelling

189 in the same and different directions. The total number of events was then divided by

190 the number of images as in the video analysis.

191 **(d) Interactions between worms: duration**

192 *(i) Experimental videos*

193   We calculated the mean duration of polarization interactions for each of the 11

194   videos also analysed for interaction frequency. We analysed a maximum of 20 such

195   interactions from each video. A random number generator was used to select 20 if

196   more had been recorded. The video was restarted at the beginning of each

197   interaction and followed through to its end. We calculated each interaction duration

198   as the difference between its start and end frame number.

199   *(ii) Simulation of non-interacting worms*

200   We mimicked the procedure with the videos of real worms as described in **(d)** *(i)* with

201   simulations of non-interacting worms. We scrolled through the bitmaps until

202   polarization events were found, and then followed the event from the first to the last

203   image in which it occurred. The number of bitmaps featuring the event was used to

204   produce the event duration in seconds based on the bitmap interval of 500ms. We

205   thus found the mean event duration for the simulation corresponding to each video.

206   **(e) Interactions between worms: aggregation formation**

207   *(i) Experimental videos*

208   We analysed all 14 videos to examine worm clustering (figure 1*e*). Using ImageGrab

209   we took a screenshot from the videos every 20s. In each image the number of

210   clusters was counted. We defined clusters as occurring when two or more worms

211   were in direct contact.

212   *(ii) Simulation of non-interacting worms*

213   The cluster counts for the simulation were performed by a modified version of the

214   simulation program. The bitmaps of the simulation at 20s intervals were loaded and

215   then the programme counted the number of clusters per bitmap.

216   **(f) Circular milling as a function of density**

217   The presence or absence of circular milling was recorded in 100 x 100mm petri

218   dishes. Five were used for each of 17 dilution series making up 85 data points

219   altogether for density. The worms were pipetted with sea water into a plastic beaker

220   to produce a high density of *S. roscoffensis* worms in approximately 50ml of water.

221   This was enough to complete one dilution series as follows: 8ml was pipetted into

222   the first petri dish and then 4ml, 2ml, 1ml and 0.5ml into the second to fifth petri dish,

223   respectively. The mixture in the beaker was consistently and evenly stirred

224   throughout the pipetting process to ensure the mixture of *S. roscoffensis* and sea

225   water was as homogeneous as possible. Sea water collected from the habitat of *S.*

226   *roscoffensis* was then added to each petri dish to make the total volume of water in

227   each up to 40ml. At time zero all of the petri dishes were agitated to ensure that

228   there were no mills present at the beginning of the experiment.

229   We observed the group of petri dishes for 60min and recorded the presence or

230   absence of circular mills in each during that period. If a circular mill was seen, further

231   observation of that petri dish ceased at that time. Thus for each of the 85 density

232   values we recorded a value of 1 if at least one mill formed and a value of 0 if no mills

233   formed over the 60min-period of observation. At the end of the observations a

234   photograph was taken of the most dilute dish of each series and the number of *S.*

235   *roscoffensis* worms was counted with ImageJ. The numbers in the other petri dishes

236   were estimated from the number counted in the most dilute dish.

237 With worms collected at the same field site as described above but in June 2015, we

238 studied the directionality of circular milling by again video-recording them in plastic

239 arenas. These data were also used in our analysis of the possible effect of arena

240 walls on the formation of circular mills (figure S5).

241 **(g) Simulation of interacting worms**

242 The simulation took place in a circular arena containing $N \le 10000$ worms placed

243 initially at random. Each worm consisted of a pair of jointed rods each 5 units long

244 with an angle between them up to +/-0.05 rad. At fixed time intervals dt the worm

245 was advanced by a distance $s = v\, dt\, (1-gc)$ along its circumscribed circle, where v

246 was the worm's standard straight-line speed, c its instantaneous curvature and g a

247 constant describing how the worm slows when turning. The final angle of the head

248 section was then chosen from the existing one and four alternative random

249 directions within +/-0.15 rad of the tail direction and on the basis of which of these

250 five options best accommodated the head with respect to the heads and tails of

251 neighbouring worms.

252 For each candidate position of the head, we calculated the energy $U = \Sigma\, \lambda\, u(r)$ where

253 the summation was taken with respect to the head and tail positions of all other

254 worms within r_{max} and r was the relevant separation (figure S4). We used an

255 approximation of the Lennard-Jones model for pair-wise interaction (figure 3*a*), as

256 commonly used in such simulations [1]:

257 $\qquad\qquad u(r) = 1 - 2r/r_{min} \qquad\qquad\qquad r < r_{min}$

258 $\qquad\qquad\quad = - (r_{max}-r)/(r_{max}-r_{min}) \qquad r_{min} \le r \le r_{max}$

259 $\qquad\qquad\qquad = 0.0 \qquad\qquad\qquad\qquad r > r_{max}$

260 The multiplier λ took the value 1.0 for head-tail calculations. For head-head

11

261 calculations we used λ = 0.5 if the tails of the two worms were separated by more

262 than the length of a worm, otherwise λ = 2.0. This weighting factor favoured

263 polarized (head-to-head) alignment. The lowest of these energies was adopted for

264 the new head position.

265 After each set of recalculations, the worms' identification numbers were shuffled to

266 avoid undue influence by any one of them, and a simple reflection procedure

267 ensured that worms stayed within the arena.

268 The values adopted for the various constants had been based where possible on

269 measurements on real worms and translated into the artificial arena (figure S4).

270 The circular arena had a radius of 200 units and given that the virtual and real worms

271 had a length of 10 units and on average 1.68mm, respectively, this represented an

272 arena of radius 33.6mm and an area of 3547mm^2.

273 We used the same simulation model in our analysis of the effect of arena boundaries

274 on the formation of circular mills (figure S5).

275 **3. Results**

276 **(a) Characteristics of individual worms**

277 The worms in our samples had a mean length of 1.68mm (SE = 0.075mm, N=57)

278 with the smallest being 0.54mm and the largest 2.91mm long. Their speed was well

279 within the distribution measured by other methods in earlier studies [9]. It increased

280 significantly with length but rather weakly and there was much variation (figure S1).

281 At low density in the circular arenas, the convoluted trajectories of individual worms

282 (figure 1*a*) were significantly biased towards clockwise movements (33 in a sample

283 of 41, Binomial two-tailed test, p = 0.0001; figure S2). Their speed declined markedly

284 as a function of body curvature (figure S3*a,b*) which in turn set their future

285 trajectories (figure 1*a*).

(b) Interactions between worms

287 To test if the worms have a tendency to interact with one another, we compared the

288 paired videos of the real worms and the simulations of non-interacting and non-

289 laterally-biased worms to determine if the real worms have either more or fewer

290 interactions than the purely random encounters of the simulated worms. This

291 comparison revealed that the real worms actively interact with one another even at

292 rather low densities (figure 1*c*).

293 We considered two or more worms to be potentially interacting, either in the

294 experimental videos or in the simulations, when they were less than 1mm apart.

295 Indeed, when this condition is met, typically the worms might be crossing over one

296 another or swimming in the same direction with their bodies in parallel (the latter

297 included worms that were closely following one another, as if in tandem). Such

298 parallel similarly orientated movement, either side by side or following, is known as

299 polarization [18].

300 The worms interacted with one another disproportionately more frequently as their

301 density increased (figure 1*b*). The durations of individual polarization events

302 increased with worm density among the real but not among the virtual worms in the

303 null model simulation (figure 1*d*). As densities increased, several of the worms

304 became involved in the same polarization interaction. In this way, they began to form

305 small cohesive fleets, which we call flotillas (figure 1*b*).

13

306   Real worms maintained contact with one another so frequently with increasing

307   densities that counting the number of isolated objects (single worms plus groups of

308   touching worms) in freeze frames of experimental videos vs. simulations showed a

309   significant difference in the numbers of observed discrete entities (figure 1*e*). In

310   short, there were significantly fewer (but bigger) aggregations among the real worms

311   than among the virtual worms because they associated more with increasing density.

312   **(c) Circular milling and directionality as a function of density**

313   The separate experiments with different densities of worms in the 100 x 100mm petri

314   dishes showed that the likelihood of circular milling in *S. roscoffensis* (figure 2*a*)

315   increases abruptly as a function of increasing density (figure 2*b*). When they began

316   to form, the initial diameter of these circular mills was on the order of about 10mm

317   and they were often well away from the dish edge (figure 2*c*). If anything, they are

318   more likely to form near the centre (figure S5). Thus, the circular milling of these

319   worms does not occur because they are responding to the boundaries of their arena

320   as a template; rather they occur because the worms are influencing one another's

321   movements.

322   Our observations from June 2015 showed that out of 45 circular mills all but one

323   were clockwise.

324   **(d) Simulation modelling of interacting worms**

325   *S. roscoffensis* worms may only be able to detect one another at very short

326   distances. Hence, we produced a new computer simulation of these worms'

327   movements with only very local interactions between them (figures 3*a* & S4) to

328   determine how the observed phase transitions, that is from solitary worms, to

329 polarized flotillas, to large circular mills might occur through self-organization [17].

330 Because we knew the size and speed of the real worms (figure S1) and the effect of

331 curvature on their speeds (figure S3), there were few arbitrary parameters. We

332 observed flotillas and milling (figure 3*b*) with reasonable choices for the elapsed time

333 per iteration, the maximum range of any interaction and the separation at which the

334 potential energy is at a minimum (figures 3*a* & S4). The likelihood of milling after a

335 given time interval as a function of N (figure 3*c*) was similar qualitatively to the

336 experimental data (figure 2*b*).

337 The behavioural lateralization of individual worms is likely to promote the probability

338 of circular milling at lower densities (figure 3*c*).

339 **4. Discussion**

340 Through cycles of experimentation and modelling we have been able to demonstrate

341 how individual worms move at low densities, how they begin to interact with one

342 another and how with increasing density this leads to circular milling behaviour.

343 The worms propel themselves through the action of cilia on their surface. However,

344 they also have muscles that determine the curvature of their bodies and hence the

345 curvature of their trajectories [8]. Such small average changes in speed with length

346 may occur because drag will be proportional to surface area, as is the number of

347 cilia, whose combined power combats such drag [27]. This might explain why worms

348 of different sizes, but all of similar proportions, move at surprisingly similar speeds.

349 Clearly, the behaviours leading to circular mill formation begin to be seen even at

350 fairly low densities; namely worms influencing one another's movements to form

351 lasting parallel formations and aggregations. Such social behaviour becomes ever

352   more common with increasing worm density (figure 2*b*).

353   The rather constant average speeds of the worms, despite substantial differences in

354   body lengths (figure S1), and their tendencies to turn in the same clockwise

355   directions (figure S2) seem to be adaptations that favour circular milling (figure 3*c*).

356   Individual worms exhibit behavioural lateralization such that they move in a

357   clockwise direction; the vast majority of circular mills (44 of the 45 observed in 2015)

358   have a clockwise rotation and simulations show that circular milling will occur at

359   lower densities when individual worms have the same directional biases.

360   In contrast to other organisms, such as starlings [28],[29], that show collective group

361   movements, these worms may only be able to detect one another at very short

362   distances and hence our simulations of potentially interacting worms are based only

363   on relatively local interactions between the worms. These simulations replicate the

364   circular milling seen among the real worms at relatively high densities (figure 3*b*,*c*).

365   Thus we have been able to establish how the movements of, and simple local

366   interactions between, individuals contribute to the self-organizing emergent

367   properties and phase transitions of large groups [17].

368   So far we have examined what factors favour circular milling in these plant-animals

369   from a mechanistic view point. Now we will consider its possible adaptive value.

370   Circular milling appears to be maladaptive in army ants and processionary

371   caterpillars. Furthermore, in the non-social glass prawns, where it arises under

372   environmental conditions which facilitate interaction during motion around a ring, it

373   also seems to serve no apparent purpose [23]. However, we hypothesize that, where

374   they are adaptive, circular mills may act as a positive-feedback vortex to capture the

375   highest possible local densities of organisms for protection by numbers or other

16

376   social advantages. In the case of *S. roscoffensis* considered here circular milling

377   may enable these plant-animals to form very dense biofilms or mats that allow them

378   to behave collectively as a social seaweed and colonize sandy beaches (figure

379   4*a&b*) where traditional macro-algal seaweeds would be unable to anchor a holdfast.

380   We hypothesize these mats enable the worms to stabilize their positions in pools of

381   seepage sea water on sandy beaches (figure 4*b*), by sharing a more or less

382   continuous mucous sheath. The sharing of such a relatively thick mucous sheet may

383   also enable the worms to benefit from sunlight on both of their sides at once as their

384   underside receives solar energy reflected from the substrate [8].

385   Recently it has been shown that individual *S. roscoffensis* worms move towards light

386   intensities that may be detrimental to the maximum photosynthetic rates of their

387   symbiotic algae [9]. Our findings here may help to resolve this paradox because

388   these worms are very likely to form dense aggregates at high light intensities and

389   may take it in turns to be sheltered or exposed by burrowing inside or onto the

390   surface of such social conglomerates. Such behaviour, using conspecific

391   aggregations as living shields against environmental extremes, is seen, for example,

392   in Emperor Penguins who form rotating huddles as protection against extreme

393   Antarctic winds [30], [31]. The worms are likely to find greater individual safety in

394   these hugely dense aggregations and may even be able to defend themselves

395   collectively through the mass production of dimethylsulphoniopropionate (DMSP)

396   [8],[32],[33].

397   Our demonstration of social behaviour, with multiple phase transitions, in *S.*

398   *roscoffensis* fills a missing tier in the long list of organisms in which collective motion

399   has been observed [34], [1]. We confidently predict that the diversity of organisms

400   exhibiting social collective motion, at all levels of biological complexity, will continue

401   to grow for the foreseeable future and that the importance of social behaviour as a

402   major evolutionary transition [35] will be increasingly recognized.

Ethics

403

404   All *S. roscoffensis* worms were returned to the place on the shore from where they

405   were collected after the experiments.

Data accessibility

406

Authors' contributions

409

410   N.R.F. initiated and designed the study, A.W. conducted the modelling, K.A.J.G. and

411   A.R.G. carried out the experiments, V.V. and H.P. analysed the experimental videos,

412   C.D. and M.L.G. helped with the experiments, M.C.S. provided the tracking software,

413   A.B.S.F. carried out the statistical analysis. N.R.F, A.W. and A.B.S.F. drafted the

414   paper. All authors contributed to revisions.

Competing interests

415

416   We declare we have no competing interests.

Funding

417

Acknowledgments

419

References

1. Vicsek, T. & Zafeiris, A. 2012 Collective motion. *Phys. Rep.* **517**, 71–140. (doi:10.1016/j.physrep.2012.03.004)

2. Biroli, G. 2007 Jamming: A new kind of phase transition? *Nat. Phys.* **3**, 222–223. (doi:10.1038/nphys580)

3. Helbing, D., Farkas, I. J. & Vicsek, T. 2000 Simulating dynamical features of escape panic. *Nature* **407**, 487–490. (doi:10.1038/35035023)

4. Sadati, M., Taheri Qazvini, N., Krishnan, R., Park, C. Y. & Fredberg, J. J. 2013 Collective migration and cell jamming. *Differentiation.* **86**, 121–5. (doi:10.1016/j.diff.2013.02.005)

5. Tamulonis, C. & Kaandorp, J. 2014 A Model of Filamentous Cyanobacteria Leading to Reticulate Pattern Formation. *Life* **4**, 433–456. (doi:10.3390/life4030433)

6. Bourlat, S. J. & Hejnol, A. 2009 Acoels. *Curr. Biol.* **19**, R279–R280. (doi:10.1016/j.cub.2009.02.045)

7. Keeble, F. 1910 *Plant-Animals: a Study in Symbiosis*. Cambridge: Cambridge University Press.

8. Bailly, X. et al. 2014 The chimerical and multifaceted marine acoel Symsagittifera roscoffensis: from photosymbiosis to brain regeneration. *Front. Microbiol.* **5**, 1–13. (doi:10.3389/fmicb.2014.00498)

9. Nissen, M., Shcherbakov, D., Heyer, A., Brummer, F. & Schill, R. O. 2015 Behaviour of the plathelminth Symsagittifera roscoffensis under different light conditions and the consequences for the symbiotic algae Tetraselmis convolutae. *J. Exp. Biol.* **218**, 1693–1698. (doi:10.1242/jeb.110429)

10. Deneubourg, J. L. & Goss, S. 1989 Collective patterns and decision-making. *Ethol. Ecol. Evol.* **1**, 295–311. (doi:10.1080/08927014.1989.9525500)

11. Lukeman, R., Li, Y. X. & Edelstein-Keshet, L. 2009 A conceptual model for milling formations in biological aggregates. *Bull. Math. Biol.* **71**, 352–382. (doi:10.1007/s11538-008-9365-7)

12. Ben-Jacob, E., Cohen, I., Czirók, A., Vicsek, T. & Gutnick, D. L. 1997 Chemomodulation of cellular movement, collective formation of vortices by swarming bacteria, and colonial development. *Phys. A Stat. Mech. its Appl.* **238**, 181–197. (doi:10.1016/S0378-4371(96)00457-8)

13. Sokolov, A., Apodaca, M. M., Grzybowski, B. A. & Aranson, I. S. 2010 Swimming bacteria power microscopic gears. *Proc. Natl. Acad. Sci. U. S. A.* **107**, 969–974. (doi:10.1073/pnas.0913015107)

14. Ordemann, A., Balazsi, G., Caspari, E. & Moss, F. 2003 Daphnia swarms: from single agent dynamics to collective vortex formation. In *SPIE's First …*, pp.

461   172–179.(doi:10.1117/12.489033)

462   15.   Fabre Jean-Henri & Legros Georges Victor 1879 *Souvenirs entomologiques :*
463   *études sur l'instinct et les moeurs des insectes / J.-H. Fabre.* Paris: Marie
464   Léonard.

465   16.   Franks, N. R., Gomez, N., Goss, S. & Deneubourg, J. L. 1991 The blind
466   leading the blind in army ant raid patterns: Testing a model of self-organization
467   (Hymenoptera: Formicidae). *J. Insect Behav.* **4**, 583–607.
468   (doi:10.1007/BF01048072)

469   17.   Camazine, S., Deneubourg, J. L., Franks, N. R., Sneyd, N. R., Theraulaz, G. &
470   Bonabeau, E. 2001 *Self-organization in biological systems (Princeton Studies*
471   *in Complexity)*. Princeton: Princeton University Press.

472   18.   Soria, M., Freon, P. & Chabanet, P. 2007 Schooling properties of an obligate
473   and a facultative fish species. *J. Fish Biol.* **71**, 1257–1269. (doi:10.1111/j.1095-
474   8649.2007.01554.x)

475   19.   Bazazi, S., Pfennig, K. S., Handegard, N. O. & Couzin, I. D. 2012 Vortex
476   formation and foraging in polyphenic spadefoot toad tadpoles. *Behav. Ecol.*
477   *Sociobiol.* **66**, 879–889. (doi:10.1007/s00265-012-1336-1)

478   20.   Couzin, I. D., Krause, J., James, R., Ruxton, G. D. & Franks, N. R. 2002
479   Collective memory and spatial sorting in animal groups. *J. Theor. Biol.* **218**, 1–
480   11. (doi:10.1006/yjtbi.3065)

481   21.   Couzin, I. D., Krause, J., Franks, N. R. & Levin, S. A. 2005 Effective leadership
482   and decision-making in animal groups on the move. *Nature* **433**, 513–516.
483   (doi:10.1038/nature03236)

484   22.   Calovi, D. S., Lopez, U., Ngo, S., Sire, C., Chaté, H. & Theraulaz, G. 2014
485   Swarming, schooling, milling: Phase diagram of a data-driven fish school
486   model. *New J. Phys.* **16**. (doi:10.1088/1367-2630/16/1/015026)

487   23.   Mann, R. P., Perna, A., Strömbom, D., Garnett, R., Herbert-Read, J. E.,
488   Sumpter, D. J. T. & Ward, A. J. W. 2013 Multi-scale inference of interaction
489   rules in animal groups using Bayesian model selection. *PLoS Comput. Biol.* **9**,
490   e1002961. (doi:10.1371/journal.pcbi.1002961)

491   24.   Hamilton, W. D. 1971 Geometry for the selfish herd. *J. Theor. Biol.* **31**, 295–
492   311. (doi:10.1016/0022-5193(71)90189-5)
493   25.   Schneider, C. A., Rasband, W. S. & Eliceiri, K. W. 2012 NIH Image to ImageJ:
494   25 years of image analysis. *Nat. Methods* **9**, 671–675.
495   (doi:10.1038/nmeth.2089)
496   26.   Stumpe, M. 2012 AnTracks.
497   27.   Alexander, R. M. 1970 *Functional design in fishes*. London: Hutchinson
498   University Library.
499   28.   Cavagna, A., Cimarelli, A., Giardina, I., Parisi, G., Santagati, R., Stefanini, F. &
500   Viale, M. 2010 Scale-free correlations in starling flocks. *Proc. Natl. Acad. Sci.*
501   *U. S. A.* **107**, 11865–11870. (doi:10.1073/pnas.1005766107)

502 29. Pearce, D. J. G., Miller, A. M., Rowlands, G. & Turner, M. S. 2014 Role of
503   projection in the control of bird flocks. *Proc. Natl. Acad. Sci.* **111**, 10422–
504   10426. (doi:10.1073/pnas.1402202111)

505 30. Ancel, A., Visser, H., Handrich, Y., Masman, D. & Maho, Y. Le 1997 Energy
506   saving in huddling penguins. *Nature*. **385**, 304–305. (doi:10.1038/385304a0)

507 31. Gerum, R. C., Fabry, B., Metzner, C., Beaulieu, M., Ancel, a. & Zitterbart, D. P.
508   2013 The origin of traveling waves in an emperor penguin huddle. *New J.*
509   *Phys.* **15**. (doi:10.1088/1367-2630/15/12/125022)

510 32. Raina, J.-B. et al. 2013 DMSP biosynthesis by an animal and its role in coral
511   thermal stress response. *Nature* **502**, 677–80. (doi:10.1038/nature12677)

512 33. Wolfe, G. V, Steinke, M. & Kirst, G. O. 1997 Grazing-activated chemical
513   defence in a unicellular marine alga. *Nat.* **387**, 894–897. (doi:10.1038/43168)

514 34. Sumpter, D. J. T. 2010 *Collective animal behaviour*. Princeton University Press.

515 35. Maynard Smith, J. & Szathmary, E. 1995 *The major transitions in evolution*.
516   Oxford University Press.

517
518
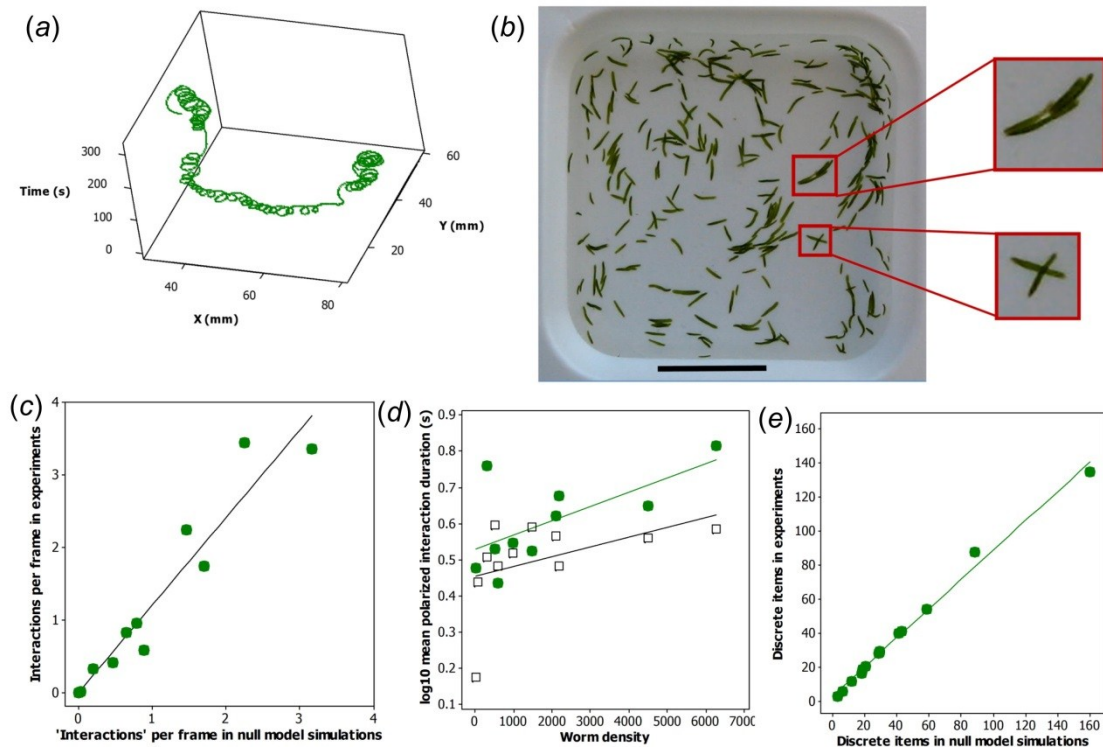
519
520 **Figure 1.** Movement of individual *S. roscoffensis* worms and behaviour at
521 intermediate densities. (*a*) Convoluted trajectory of a single worm. This individual
522 made predominantly clockwise movements. (*b*) Flotilla formation at intermediate
523 densities. The black scale bar at the bottom of the arena represents 10mm. The
524 upper red square shows a polarized group of 4 worms moving in the same direction
525 in mutual contact (i.e. a flotilla; see also the upper panel to the right). The lower red
526 square shows two worms crossing over one another (see also the lower panel to the
527 right). (*c*) Comparison between number of interactions (per frame, both crossings
528 and polarizations, see Material and methods) among worms in experimental videos
529 and number of crossing and polarization events (per frame) in paired null model
530 simulations at low to intermediate densities. The line of best fit passes through the
531 origin and has a slope = 1.205 (t_9 = 15.44, p < 0.001), which is significantly greater
532 than 1 (95% CI: 1.029, 1.381; see ESM). Thus, there are more interactions between
533 the real than between the virtual worms. (d) Polarized interaction durations increased
534 among real worms in the experiments (green circles) but not among the virtual
535 worms in the null model simulations (empty squares) which are paired with each
536 experimental video (N=11). The gradient of the relationship between $\log_{10}$ mean
537 polarization event duration (s) and worm density is significantly different from 0 for
538 the videos (slope = 0.000040, t_8 = 2.44, p = 0.040), but not for the null model
539 simulations (slope = 0.000027, t_9 = 1.53, p = 0.161). This means that the relationship
540 between polarization event duration and density (see ESM) can be attributed entirely
541 to the data from the worms in the experiments. (*e*) The worms aggregate more in the
542 experimental videos than in the null model simulations with increasing density as
543 shown by the slope of the regression line being significantly less than 1. (N=14; data
544 from 13 circular arenas and 1 densely populated square arena (the latter is
545 represented by the point at the top right.) Thus there are fewer discrete objects in the
546 videos than in the paired null model simulations. The equation of the line is: No. of

547 discrete items in experiments = 3.19 + 0.858 No. of discrete items in simulations (R^2
548 = 99.2%). The slope is significantly different from 0 (t_{12} = 38.73, p < 0.001) and
549 significantly smaller than 1 (95% CI: 0.810 - 0.906; 99% CI: 0.790 - 0.925; see ESM).
550
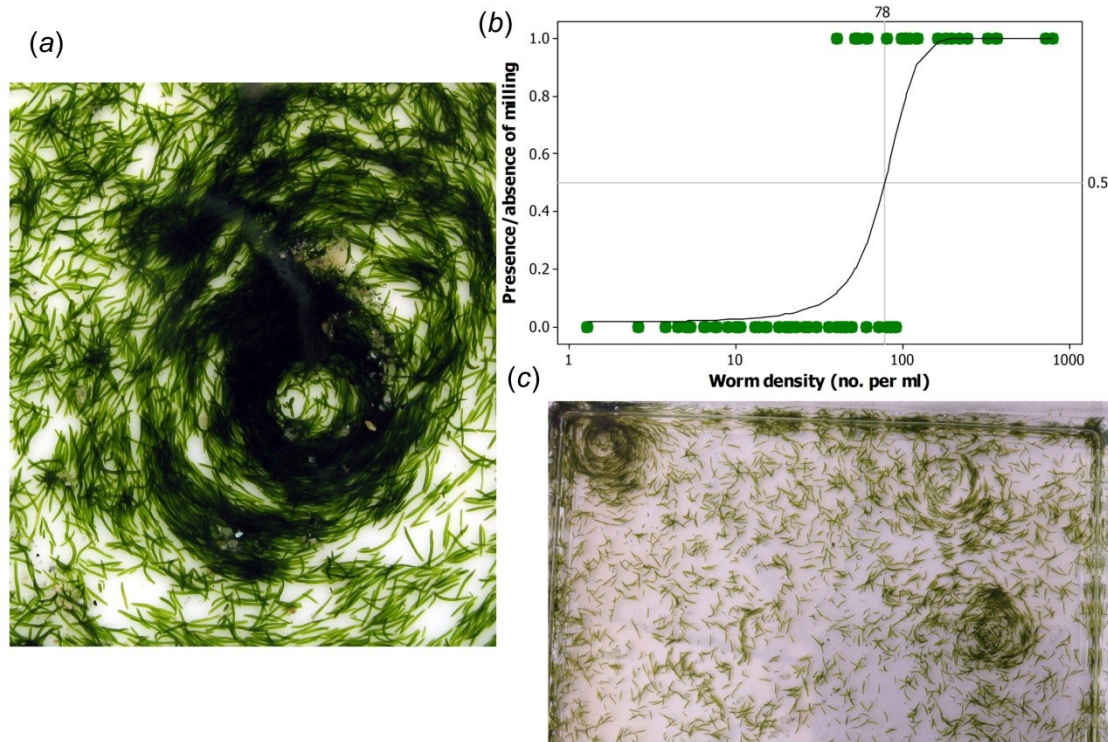
551
552 **Figure 2.** *S. roscoffensis* worms exhibit milling as a step function of increasing
553 density. (*a*) A circular mill in a small arena. (*b*) The relationship between worm
554 density (no. per ml) and the presence or absence of circular mills (1 and 0,
555 respectively); green circles: data, black line: predicted probabilities from the fitted
556 binary logistic regression model log(π/(1-π)) = -4.126 + 0.053*x*, where π is the
557 probability of milling and *x* is worm density. The model predicts that with every
558 additional worm per ml the probability of milling increases on average by 5% (95%
559 CI: 3 – 8%) and that at density above 78 worms/ml, the presence of milling becomes
560 more likely than not (see ESM). (*c*) Part of a 100 x 100mm perti dish where three
561 circular mills have formed.
562
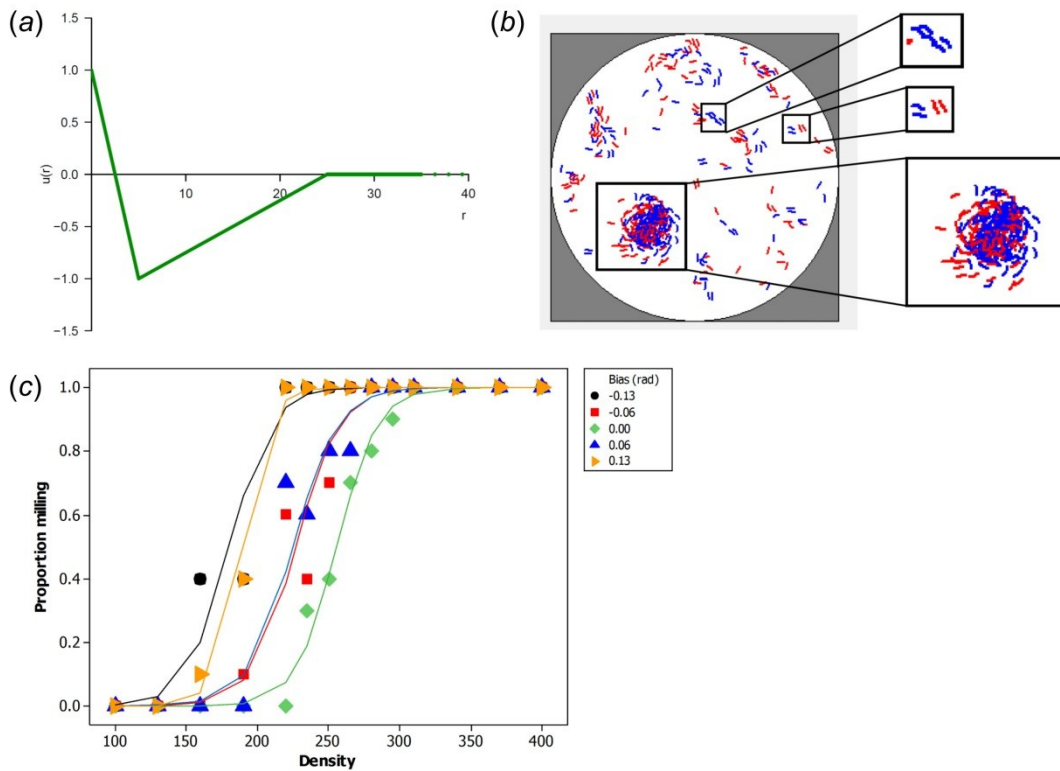
Figure 3. Simulation of interacting worms. (*a*) Potential energy curve, an approximation of the Lennard-Jones model [1], used for pair-wise interactions in the simulation of interacting worms; u(r): potential energy function, u(r) > 0: repulsion; u(r) < 0: attraction; r: range of interaction; at r_{min} = 5 attraction is at its maximum and r_{max} = 25 is the maximum range for any interaction (see figure S4 for pseudocode). (*b*) The results of one simulation showing one circular mill (lower panel) and several flotillas (examples in the top two sub-panels; worms in blue or red are temporarily moving clockwise or anticlockwise, respectively; note, these simulations have neither left not right biases in the movements of individual worms). (*c*) Self-organizing circular mills in the simulations as a function of density for different levels of lateral bias (rad) in the movement of individual worms; the bias range -0.13 to 0.13 rad goes from clockwise to anticlockwise with 0.00 rad representing no bias. There was a significant effect of density on the proportion of simulations with milling (out of 10 simulations for each value of density); note density here (i.e. the number of worms per simulation arena) cannot be directly compared to density of the real worms in a volume of sea water. For each of the five levels of bias, the proportion of simulations with milling increased by 7% (95% CI: 6 – 9%, p < 0.001, see ESM) with every additional worm. However, the inflection points differed; the inflection point for no bias (0.00 rad) was significantly different from the other four while the inflection points for clockwise and anticlockwise biases of the same magnitude (-0.13 and 0.13 rad or -0.06 and 0.06 rad) were not significantly different from each other and significantly different from the rest (table S1).
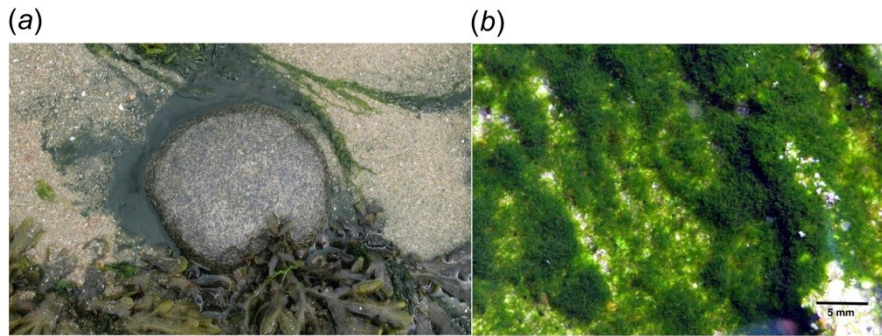
587
588 **Figure 4.** Dense mat formation of *S. roscoffensis* on a Guernsey beach. *(a)* The
589 worms are in the drainage channel (from 7 to 2 o'clock) around the circular rock
590 which is approximately 15cm across. The rock is an anchor for the holdfasts of the
591 macro-algae in the photograph, whereas the worms will burrow into the sand on the
592 incoming tide. *(b)* A close-up of a mat revealing heterogeneity in worm density.
593